

國立臺灣大學醫學院暨工學院醫學工程學研究所

碩士論文

Graduate Department of Biomedical Engineering

College of Medical and College of Engineering

National Taiwan University

Master Thesis



受電場而極化的脂膜筏引導纖維母細胞之方向性移動

Electric Field-induced Lipid Raft Polarization Guide

Fibroblast Directional Migration

林栢江

Bo-Jiang Lin

指導教授：趙本秀 博士

Advisor: Pen-Hsiu Grace Chao, Ph.D.

中華民國 102 年 7 月

July, 2013



國立臺灣大學碩士學位論文
口試委員會審定書

受電場而極化的脂膜筏引導纖維母細胞之方向性移動
Electric Field-induced Lipid Raft Polarization Guide
Fibroblast Directional Migration

本論文係林栢江君 (R00548052) 在國立臺灣大學醫學工程學研究所完成之碩士學位論文，於民國 102 年 07 月 19 日承下列考試委員審查通過及口試及格，特此證明

口試委員：

趙平

(指導教授)

趙玲

李偉博

所長：

王北麟

序言



工業技術與醫學知識的對撞，激盪出宣示未來新希望的煙火，也散發著那使我著迷的炫彩，而臺灣大學醫學工程所給予了我一個契機，讓我得以參與這歷史的進程，最要感謝的人，是指導我何謂科學家思維的教授—趙本秀老師，「要對 data 忠心」正闡述著趙老師對於假說的嚴謹，也是其要求麾下研究生應有的態度，兩年碩士班生涯走過，也因有宋承修和曾筱筠的陪伴才能如此順遂與歡樂，好夥伴的相互扶持，已畢業的鄭祐甄、蔡承憲、馮嘉襄、徐向儀、沈守謙和張維仁的教導，讓我學習到待人處事上的眉角，也感謝博士班學長溫新民的坐鎮，讓 lab501 運轉率百分百；Jeff 除了是個有品味的飯友也是英文會話的家教；已提早退席的游婉婷著實地讓平凡生活增加不少趣事，此外，也感謝王兆麟老師麾下的崔哲豪、王彥凱、陳志維以及徐于鈞等人平日增添本實驗室風采之外，也讓我跟隨順道拜訪夏威夷的國際會議團，一路上除了驚險萬分也是收穫滿分，本論文得以完成則有泰半來自生命科學院核心實驗室莊以君的體諒，才能有著高品質的 confocal 螢光照片，還有醫學院第一共同研究室許華蔓的操作，才得順利在 ORS 上發表不同種類電場如何影響細胞的論文，也感謝暑期研究生何玉樺辛苦量化 lipid raft 的分佈和 Alex 熬夜撰寫的 lipid raft 模擬程式，使本論文更加完整，因為有了過去的你們，才成就了現在的我，由衷感謝。

摘要



當微生物或細胞受到電場影響而展現出順著電場方向移動，此為趨電性。許多研究指出膜蛋白的分佈狀況會影響趨電性的行為，在先前的研究中指出 $\alpha 2\beta 1$ integrin 受電場影響而有極化的現象，且其在交流電與直流電刺激中有著相反的分佈情形，因此本研究想探討細胞膜上的微結構—脂膜筏，在纖維母細胞受交流電或直流電影響後，如何控制細胞的移動性，結果中發現，脂膜筏受電場影響而聚集，且跟 $\alpha 2\beta 1$ 素蛋白有著相似的分佈，此外，九成的 $\alpha 2\beta 1$ 素蛋白坐落在脂膜筏上，如果破壞脂膜筏會抑制纖維母細胞的趨電性行為，另外，抑制 caveolin-1 的基因表現也會抑制往負極向移動和 RhoA 的分佈，因此從本研究的研究中，可以知道脂膜筏會藉由 caveolin-1 影響纖維母細胞趨電性的表現。

關鍵字：脂膜筏、素蛋白、細胞移動、電場、趨電性

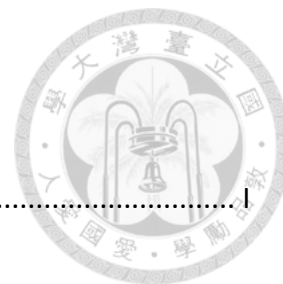
Abstract



Galvanotaxis is a phenomenon in which microorganisms migrate in response with the electric current. Most studies indicate that the redistribution of plasma membrane proteins guides cell directional motility. The previous study showed that $\alpha 2\beta 1$ integrin polarizes with AC and DC electric fields. This study shows when fibroblasts are stimulated by an electric field, lipid rafts polarize and the polarization coincides with asymmetrically-distributing $\alpha 2\beta 1$ integrins. Disruption of lipid rafts inhibits EF-induced directional migration. The caveolin-1 knockdown inhibits cell directional motility and RhoA polarization. The results indicate that lipid raft is a mechanosensor to EF stimulation and lipid raft polarization lead to integrin and caveolin-dependent directional migration.

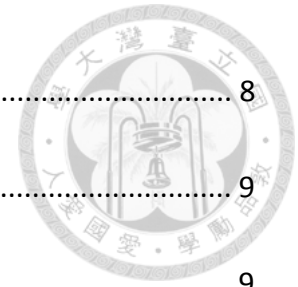
Key Words: lipid raft, integrin, migration, electric field, galvanotaxis

Contents



口試委員審定書	I
序言	II
摘要	III
Abstract.....	IV
List of Tables	VII
List of Figures.....	VII
Chapter 1. Introduction	1
Chapter 2. Materials and Methods	5
2.1 Primary Porcine Fibroblasts Culture	5
2.2 Microfluidic channel Fabrication	5
2.3 RNA interference.....	6
2.4 Pharmacological Treatment	7
2.4.1 Cholesterol Depletion.....	7
2.4.2 Plasma Membrane Solidification.....	7
2.4.3 Integrin functional block	7
2.5 Electric field stimulation	7
2.6 Fibroblast Behavior Quantification	8
2.7 Lipid Raft Labeling	8

2.8	Reverse Transcription Polymerase Chain Reaction.....	8
2.9	Immunofluorescence staining.....	9
2.10	Image Analysis	9
2.11	Statistics.....	10
Chapter 3.	Results	11
3.1	EF-induced lipid raft redistribution	11
3.2	Caveolin-1 signaling pathway	12
Chapter 4.	Discussion.....	14
Reference.....		34



List of Tables

Table 1. Primers used in this study (Primer-BLAST, NCBI)	17
Table 2. siRNA for caveolin-1 (Qiagen).....	18



List of Figures

Figure 1. Galvanotaxis Chamber (Cannizzaro et al. 2009).	19
Figure 2. Microfluidic Channel.	20
Figure 3. Directionality and Asymmetry Index.....	21
Figure 4. Lipid raft polarization	22
Figure 5. Coincide between lipid raft and $\alpha 2\beta 1$ integrin.....	23
Figure 6. $\alpha 2\beta 1$ integrin riding lipid raft.....	24
Figure 7. Lipid raft polarization disrupt by Ch and M β CD.....	26
Figure 8. Ch and M β CD impair galvanotaxis	27
Figure 9. Cav1 polarize under electric field stimulation.	29
Figure 10. Cav1 knockdown by RNAi.	30
Figure 11 Caveolin-1 knockdown disrupt $\alpha 2\beta 1$ integrin distribution	31
Figure 12. Cav1 knockdown reduce directionality.....	32
Figure 13. RhoA polarization induced by EF is impaired by RNAi.	33

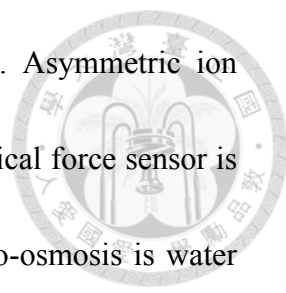
Chapter 1.

Introduction



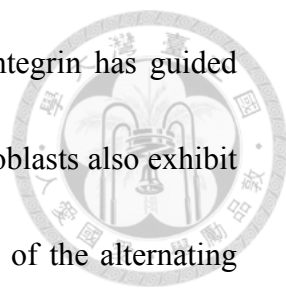
Most studies indicate that endogenous electric currents advanced the nerve regeneration and facilitate the wound healing [1-3]. While epithelia are injured, trans-epithelial potentials (TEP, [4]) on the wound drops and the potential differences drive the electric current toward the wound center. For example, an electric field measured 42mV/mm in cornea wound and an electric current generated $10 \mu\text{A}/\text{cm}^2$ at peak, persisted at $4 \mu\text{A}/\text{cm}^2$ in human skin [4, 5]. That migration of cell in response to an electric field is a phenomenon, called galvanotaxis or electrotaxis. Galvanotaxis was first observed on leukocytes by Dineur in 1891. The displacement of a cell depends on current density, voltage, and solute in the medium. Besides that, cell morphology will change under electric field. For example, fibroblasts not only increased speed and directionally migrated toward anode but also rearranged cytoskeletons perpendicular to electric currents and elevated the ECM-related gene expression, like type I collagen, while exposed on electric field [1, 6]. Consequently, many studies have attempted to delineate the mechanisms how cells sense an electric field.

Due to the high impedance of plasma membrane, how electric field sensing mechanism is following on four physical hypotheses: asymmetric ion flow,



mechanical force sensor, electro-osmosis and electrophoresis [7]. Asymmetric ion flow is that the ion redistribution induced by electric field. Mechanical force sensor is that charge membrane channels open gate by electric field. Electro-osmosis is water potential owing to plasma membrane attracting ion. Electrophoresis is that charge particles move along the electric field. Recently studies reveal that the behavioral response to electric field is attributed to the polarization of plasma membrane molecules [8]. Some plasma membrane proteins, like integrin and EGF receptor, are founded to asymmetrically distribute under electric field [9, 10]. Impaired the function of integrin can disrupt the directional motility of cells [9]. Integrin, a heterodimer containing an α and a β subunit, is a major families of cell adhesion. Its function can be divided into two parts. One is to assembly with cytoskeleton and signal molecules, like PI3 kinase and FAK [7, 11]. The other is to combine with extracellular matrix as a focal adhesion, a main component of cell adhesion and migration [12, 13]. Therefore, spatial downstream signaling pathway activated by integrin is a hub to reveal the intrinsic mechanism of galvanotaxis.

Rho family of small GTPase, including Rho, Rac1 and Cdc42, is G-protein which transits the extracellular message as a cellular signal molecule [14]. While migrating, cell protrude their actin-based lamellipodium, where integrin-based adhesion activate RhoA [15]. RhoA-related contract leads cells to the orientation into



which lamellipodia project [16]. Polarized distribution of $\alpha 2\beta 1$ integrin has guided ligament fibroblasts via RhoA in our previous study. However, fibroblasts also exhibit polarization in applied AC fields, despite the asymmetrical nature of the alternating current. It implies that a small structure with fast response time (half the applied 60Hz duration) can initiate the mechanism to polarize integrin and direct cell migration.

“Membrane rafts are small (10–200 nm), heterogeneous, highly dynamic, sterol- and sphingolipid-enriched domains that compartmentalize cellular processes. Small rafts can sometimes be stabilized to form larger platforms through protein-protein and protein-lipid interactions” report by Pike [17]. Lipid raft is a key structure for endocytosis [18], membrane traffic [19] and cell migration [20]. The property of lipid raft is to cluster into huge while stimulated [21]. Some reports show that integrin activating by ECM cluster on lipid raft [19]. The impairment of the lipid raft inhibits the polarization of integrin [22]. Lipid raft contains caveolin-1, which interact with different membrane protein-related signaling pathway and form a caveolae [23]. For example, caveolin-1 bind with $\beta 1$ integrin to activate RhoA though inactivation of p190RhoGTPase [24]. The caveolin-1 also control the $\beta 1$ integrin activation though Cbp-Csk-Src pathway while forming the caveolin-1/ $\beta 1$ integrin complex [25]. Studies indicate that caveolin-1 is crucial for directional migration by activation RhoA [26, 27]

Therefore, we hypothesize that lipid raft taking $\alpha 2\beta 1$ integrin clusters on the leading edge of migration direction and guides cells to respond to electric fields through caveolin-1. In this thesis, we aim to figure out the role of lipid raft in galvanotaxis and understand the function of lipid raft on the integrin-dependent RhoA signaling pathway. The results showed that depletion of lipid raft resulted in the loss of oriented motility but no significant change of speed. It also impaired the polarized distribution of integrin. The knockdown of caveolin-1 disrupted galvanotaxis. We delineated a brief EF-induced cell signaling pathway, which lipid raft was an electric currents sensing unit and a complex combined with integrin to activate RhoA.

Chapter 2.

Materials and Methods



2.1 Primary Porcine Fibroblasts Culture

Anterior cruciate ligament fibroblasts were harvested from young porcine knee joints. Anterior cruciate ligament (ACL) wash in PBS then is torn into pieces. The explants were cultured in 3cm dishes with 4.5 g/L D-glucose DMEM with 10% FBS (Invitrogen), 1% penicillin/streptomycin (Gibco) and 1% HEPES (Biowest), under 37 °C incubator with 5% CO₂. Growth media were changed every 3 day until confluence. For electric field stimulation studies, ACL fibroblasts were resuspended by 2 min incubation with 0.25% trypsin-EDTA (Gibco) and seeded on the microfluidic channel at 4×10^5 cells/cm² or on sterile glass slides at 4×10^4 cells/cm² for 2 hours in incubator. The slides combined with a galvanotaxis chamber for electric field stimulation (Figure 1).

2.2 Microfluidic channel Fabrication

The straight microchannels made of polydimethylsiloxane (PDMS) by soft lithography procedures. SU8 photo resist (Gersteltec Sarl) spread on silicon wafer by a spinning coater then exposed with UV lights though mask to develop patterns.

PDMS was molded over the SU8 master for two days then separated. PDMS channels were then cured at 70 °C overnight. After cooling, the PDMS channels were punctured for inlets and outlets and attached to glass substrate [28]. Channels are 3 mm wide, 400 μm high and 10 mm long (Figure 2). Fresh DMEM were added into microchannel every hour in case of evaporation and connect the agarose salt bridge on the poles of chamber after 2 hours incubation.

2.3 RNA interference

The RNA interference for caveoline 1 (Cav1) was performed by small interfering RNAs (siRNA) and AllStars negative siRNA modified with alexa flour 488 (Cat#1027284, Qiagen) was used as control. The siRNA, is complement to Cav1, was designed by Qiagen and the sequence is the following Table 2. ACL fibroblasts were seeded on 6-well dishes at 2×10^5 cells/well. siRNA diluted on 100μl serum-free DMEM then were mixed with 6μl HiPerFect[®] transfection reagent (Cat#301702, Qiagen) by vortexing 10 sec. After 10 minutes on siRNA mixture standing, every well was added with 150 ng si-Cav1 or 75 ng Negative Control siRNA for 2 days then washed and reseed on the sterile glass for electric field stimulation.



2.4 Pharmacological Treatment

2.4.1 Cholesterol Depletion

Cells were washed with PBS and incubated for 1 h at 37°C with serum-free DMEM of 5 mM methyl β -cyclodextrin (M β CD, Cat#C4555, sigma,[29]).

2.4.2 Plasma Membrane Solidification

Cholesteryl hemisuccinate (Ch, Cat#C6512, sigma), an analog of cholesterol, were dissolved in dimethylsulfoxide and diluted with PBS at 0.5% final concentration. Cells were preincubated with 1 mM ChH for 30 minutes then washed [30].

2.4.3 Integrin functional block

Anti-porcine integrin $\alpha 2\beta 1$ antibody (Cat#mab1998, Invitrogen, 1 mg/ml) diluted with PBS at 2.8 μ g/ml. Cells were treated with it for 30 min then washed [9].

2.5 Electric field stimulation

Constant direct current (DC) EF was applied at a field strength of 6 V/cm parallel to the microchannel direction and galvanotaxis chamber using a Keithley Source Meter and alternative current (AC) sinusoid waves (sin) was applied at a peak

intensity of 1.2 V at 50 Hz using a custom stimulator (Dynaprog, MingQuo, Taiwan).



2.6 Fibroblast Behavior Quantification

Cells were captured by Cannon EOS every 15 minutes and calculated their position by determining the centroid at the initiation and the end. The displacement and orientation were measured and represented as velocity and directionality. The directionality was described by cosine θ , where θ was the angle between the EF field axis and the cell translocation vector. $\theta = 0^\circ$ was assigned to the cathode and 180° was assigned to the anode. Therefore, the range of cosine θ was between +1 and -1 and an index of directed migration (Figure 3.a).

2.7 Lipid Raft Labeling

Alexa Fluor® 555 conjugate-cholera toxin B (CTxB, Cat#C-22843, Molecular Probes), binding to the GM1 gangliosides, was diluted with chilled complete growth medium at $1\mu\text{g/ml}$. After the EF Stimulation, channels were filled with chill complete growth medium. It was replaced with CTxB for 10 minutes at 4°C then wash. Finally, 4% formaldehyde rinse it for 30 minutes and maintain the temperature on 4°C .

2.8 Reverse Transcription Polymerase Chain Reaction

Cells were lysed by TRIzol and reverse transcription was performed by using superscriptTM III transcriptase in a thermal cycler (Bioner) and amplification was

performed by GoTaq® green master mix (Promega). The primers of caveolin 1 and GAPDH are as following Table 2 (Primer-BLAST, NCBI). Amplified cDNA fragments were resolved by electrophoresis on 2% agarose gel staining ethidium bromide. The intensity of band was detected by ultraviolet illumination, quantified by ImageJ and normalized against that of GAPDH.

2.9 Immunofluorescence staining

Upon completion of fixation, cells were permeabilized by 0.3% triton X-100 for 5 mins and blocked with 5% FBS in PBS for 1 hour after wash trice. Cells were incubated overnight in 4°C with primary monoclonal anti- $\alpha 2\beta 1$ integrin antibody (1:200, Invitrogen) or primary monoclonal anti-caveolin 1 antibody (1:200, Cytoskeleton) or primary monoclonal anti-RhoA antibody (1:200, Cytoskeleton). Goat anti-mouse alexa flour 488-conjugated antibody (1:250, Invitrogen) supplemented with 5% FBS for 1 hour and so was goat anti-rabbit alexa flour 555-conjugated antibody (1:250, Invitrogen). SlowFade® gold antifade reagent (Invitrogen) was used to mount the coverslips onto the glass slides. Slides were observed on confocal microscopy (Leica TCS SP5).

2.10 Image Analysis

Each cell was divided into four equal quadrants and the mean fluorescence

intensity was measured by an image process program developed from LabVIEW 2011 SP1 (National Instruments). Asymmetry Index (AI) was calculated by subtracting the normalized intensity of the region facing cathode from the region facing anode, and normalized to the overall average intensity of the cell. A positive value of AI indicates cathodal distribution and a negative value of AI indicates anodal distribution (Figure 3.b).

2.11 Statistics

R 3.0 (The R Foundation for Statistical Computing) was used to perform one-way ANOVA with Tukey's HSD post hoc test under $\alpha = 0.05$. Data represent mean \pm standard error.

Chapter 3.

Results



3.1 EF-induced lipid raft redistribution

In our previous study, we found that $\alpha 2\beta 1$ integrin showed different distribution between DC and AC. It is possible that lipid raft, a larger size microdomain than protein, floating on the plasma membrane carry these parallel to EF. To investigate whether lipid raft response to EF, we quantified the fluorescence intensity of cholera toxin B-labeled lipid raft distribution with time. The lipid raft polarized and coincided with $\alpha 2\beta 1$ integrin (Figure 4 and Figure 5). The $\alpha 2\beta 1$ integrin polarization is consistent with previous study. It indicated that lipid raft not only reacted to EF but also correlated with $\alpha 2\beta 1$ integrin.

To delineate the relationship between lipid raft and $\alpha 2\beta 1$ integrin, we observed the $\alpha 2\beta 1$ integrin distribution while lipid raft deconstruction and the lipid raft distribution while functional block on $\alpha 2\beta 1$ integrin. We found raft impairment caused the $\alpha 2\beta 1$ integrin randomly distribute but integrin block did not affect the lipid raft polarization (Figure 6). It indicated that $\alpha 2\beta 1$ integrin were shipped by lipid raft.

Based on our hypothesis that lipid raft can move on the plasma membrane with low-drag, we investigate the role of lipid raft distributed between on cell migration.

Pharmaceutical treatments used cholesteryl hemisuccinate to reduce membrane fluidity and methyl β -cyclodextrin to impair the lipid raft structure. Significantly, lipid rafts distribute asymmetrically when exposed to electric field and randomly when treated with these chemicals (Figure 7).

We measured the displacement and direction of fibroblasts with cholesteryl hemisuccinate and methyl β -cyclodextrin (Figure 8.a). Lipid raft disruption and membrane solidification did not vary the velocity; however, they did inhibit the directional migration induced by EF (Figure 8.b).

3.2 Caveolin-1 signaling pathway

We further investigated whether or not caveolin-1 played a role in $\alpha 2\beta 1$ integrin and lipid raft with electric field stimulation. Caveolin-1 polarized while DC electric field stimulation (Figure 9). Knockdown of caveolin-1 expression by RNAi impaired cell directionality but not impact on cell motility (Figure 10 and Figure 12). Knockdown caveolin-1 shows no effect on caveolin-1 polarization but impairs integrin distribution; however, integrin functional block shows no effect on lipid raft polarization but impairs caveolin-1 distribution (Figure 9 and Figure 11). RhoA polarization induced by electric field also disrupts while RNAi treatment and lipid raft deconstruction (Figure 13). It seems that the polarization of caveolin-1 and $\alpha 2\beta 1$ integrin coincide with quantity of caveolin-1 and function of $\alpha 2\beta 1$ integrin. The data

imply that caveolin-1 on the lipid raft could control galvanotaxis through RhoA and cooperation with $\alpha2\beta1$ integrin.



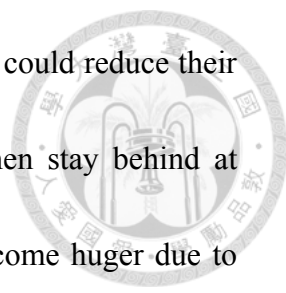
Chapter 4.

Discussion



It is evident from the results that overall, lipid rafts polarization induced by electric field guide cell migration through caveolin-1. That electric field causes the lipid rafts polarization correspond with that lipid raft can merge into large and stable structure under stimulation. The polarization of lipid raft shares a similar pattern with those of $\alpha2\beta1$ integrin. These consist with previous finding, which show that $\alpha2\beta1$ integrin polarize under electric field stimulation [9]. As previous research by Leitinger indicated, lipid raft localization are relevant to integrin cluster [22]. The $\alpha2\beta1$ integrin colocalize with lipid raft. The deconstruction of lipid raft impairs the redistribution of $\alpha2\beta1$ integrin; however, the function inhibition of $\alpha2\beta1$ integrin shows no change on the polarization of lipid raft. It is indicated that lipid raft regulate the distribution of $\alpha2\beta1$ integrin with electric field stimulation.

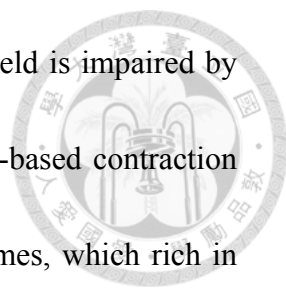
According to Hart's formula, the force from membrane, environment viscosity can affect the electric force exerting on the membrane molecules [31]. The drag force and viscous force could influence the lipid raft polarization. The larger size of lipid raft causes the higher drag force from membrane. Furthermore, the huger lipid raft can bear more plasma membrane proteins. The possible mechanism on AC sin wave



electric field is that the merge of lipid raft induced by electric field could reduce their diffusion rate. Lipid rafts gather with each other at beginning then stay behind at reverse electric field. It is reasonable that the larger lipid rafts become huger due to the possibility of their contacting with small one. As hypothesized, lipid rafts polarize at the cell area to which the initial 16ms current orient under AC sin wave electric field stimulation. The opposite initial currents compared to DC electric field determine the orientation of lipid raft redistribution. This finding reveals that lipid raft can polarize at briefly electric field exposure time.

As expected, the increase of membrane viscosity by cholesteryl hemisuccinate can inhibit the lipid raft polarization not only on AC but also on DC. Consequently, the results show that the lipid rafts size and the membrane viscosity affect lipid raft diffusion rate. Lipid raft clustering is dependent on the initial orientation of current due to the change of diffusivity.

Our results show that knockdown of caveolin-1 can impair galvanotaxis. How caveolin-1 affect cell migration is that Rey-Barroso delineates that caveolin-1 control focal adhesion and migration though activating FAK and $\beta 1$ integrin [25]. Moreover, the knockdown of caveolin-1 affect integrin polarization and functional block of $\alpha 2\beta 1$ integrin influence caveolin-1 distribution. It imply that integrin and caveolin cooperate with each other [24].



It also indicated that RhoA polarization induced by electric field is impaired by caveolin-1 knockdown and lipid raft disruption. RhoA cause actin-based contraction and lead to cell migration. RhoA is located on fibroblasts podosomes, which rich in F-actin related to cell adhesion [32]. Therefore, the RhoA location affects the cell motility. Our results show that lipid raft can affect directional migration though controlling RhoA polarization.

We find that lipid raft polarize under electric field stimulation. The polarization guides cell directional migration though caveolin-1. The initial orientation of electric current determines the area at which lipid raft distribute and the direction to which cell migrate. In future study, we would investigate the signaling mechanism of caveolin-1 and RhoA. For instance, previous research indicates that integrin/caveolin-1 complex could activate RhoA though p190 RhoGAP [24].

Table 1. Primers used in this study (Primer-BLAST, NCBI)

Primer	Sequence 5' to 3'	Annealing Temperature(°C)	Product size(bp)
GAPDH	Forward TCC CTG CTT CTA CCG GCG CT	59	281
	Reverse GCC AGC CCC AGC ATC AAA GGT		
Caveolin-1	Forward ACA TCT CTA CAC CGT CCC CA	54	181
	Reverse ACG TCG TCG TTG AGA TGC TT		



Table 2. siRNA for caveolin-1 (Qiagen)

Name	Sequence 5' to 3'	Conc. (nmol/tube)
Target	CTGGAATAAATTCAAATTCCTT	
Sense strand	GGAAUAAAUUCAAAUUCUUUU	20
Antisense strand	AAGAAUUUGAAUUUAUUC CAG	



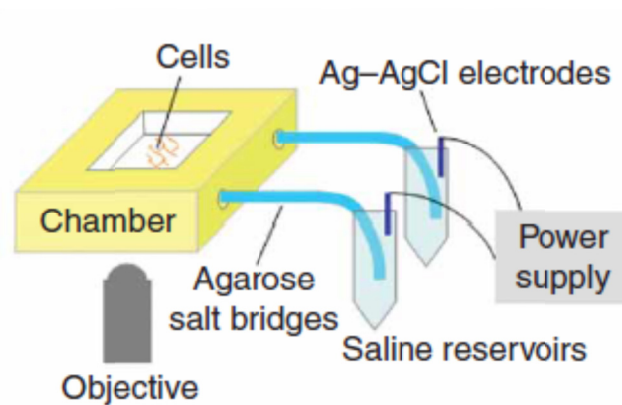
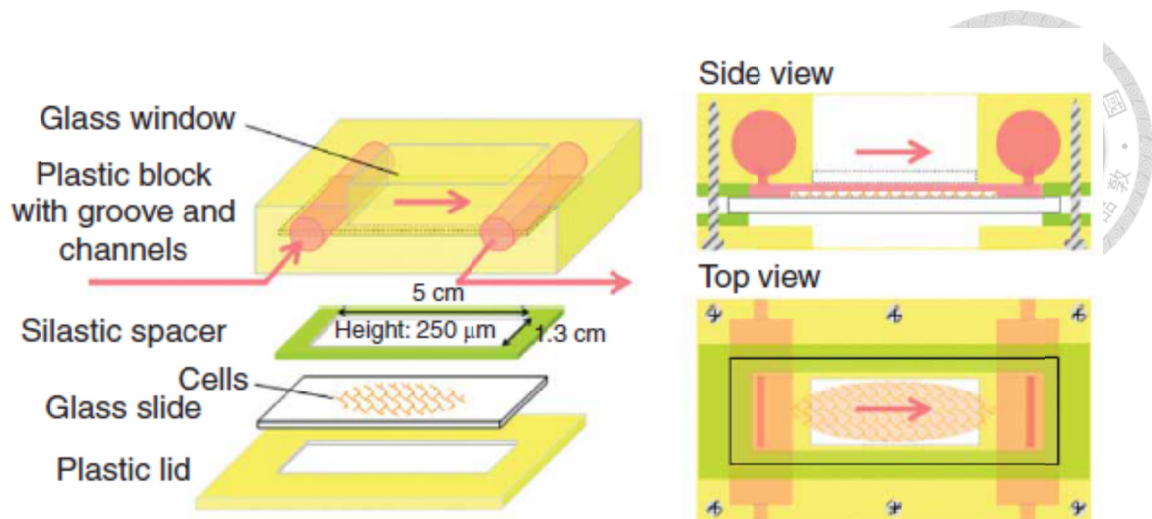


Figure 1. Galvanotaxis Chamber (Cannizzaro et al. 2009).

Cells are deposited on the center of the glass slide, which is fitted into the transparent chamber. The objectives of the phase contrast microscope observe the cell behaviors through the glass window. The channels filled with DMEM maintain cells under medium during EF stimulation and connect to saline reservoirs with 2% agarose salt bridge [33].

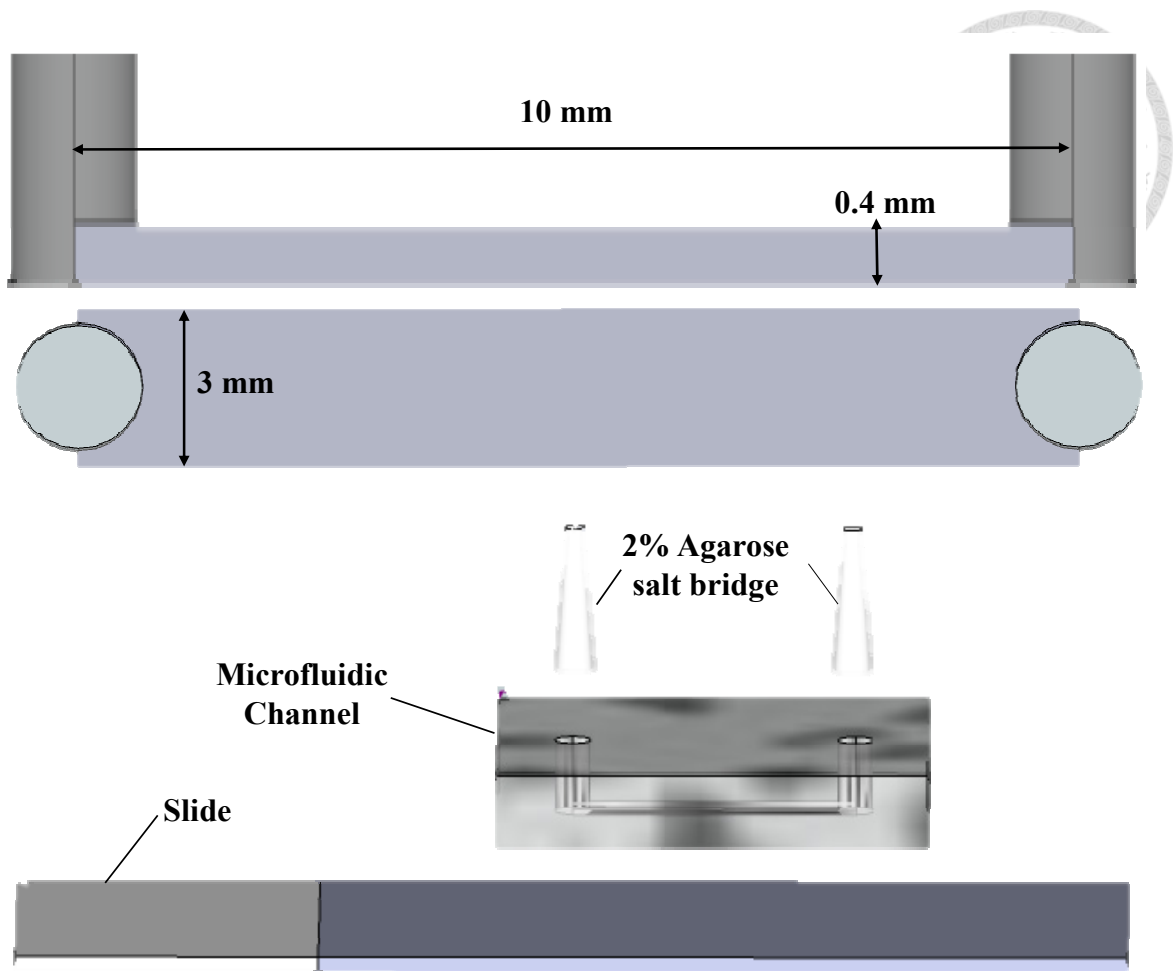


Figure 2. Microfluidic Channel.

It is made of MEMS. The channel is 0.4 mm height, 10 mm length and 3 mm width.

Two pores are punctured as an inlet and an outlet. The channel combines with glass slide and connects to power supply with 2% agarose salt bridge.

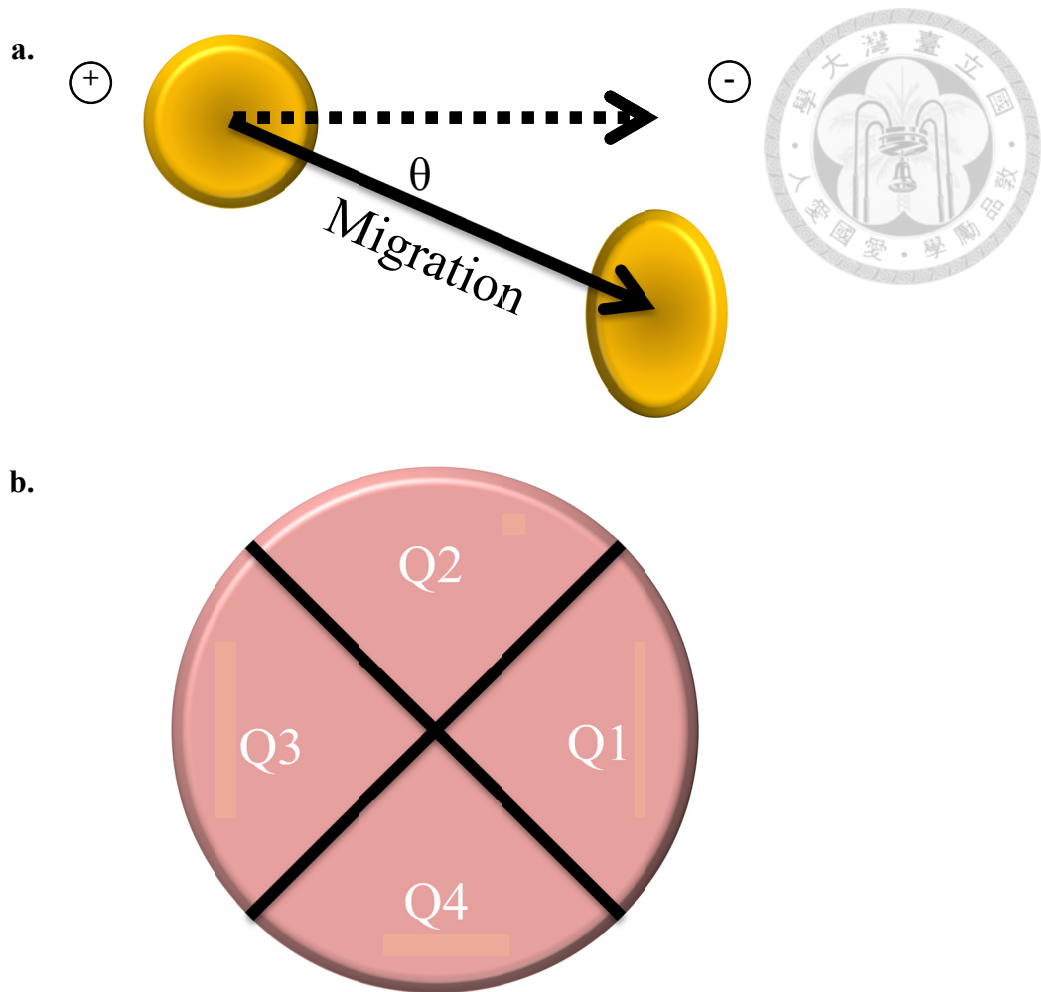


Figure 3. Directionality and Asymmetry Index

(a) The cell displacement from initiation to the end of stimulation is represented as cell migration and these projecting on the electric field axis are represented as directionality. (b) Cell is divided into four areas then the mean fluorescence intensity quantified. Q1 represent the cathodal side of cell and Q3 represent the anodal side of cell. The difference between Q1 and Q3 is a symbol of the target distribution, called asymmetric index (AI). The positive value of AI means the majority of protein cluster in the cathodal side and the negative value of AI means these clusters in the anodal side.

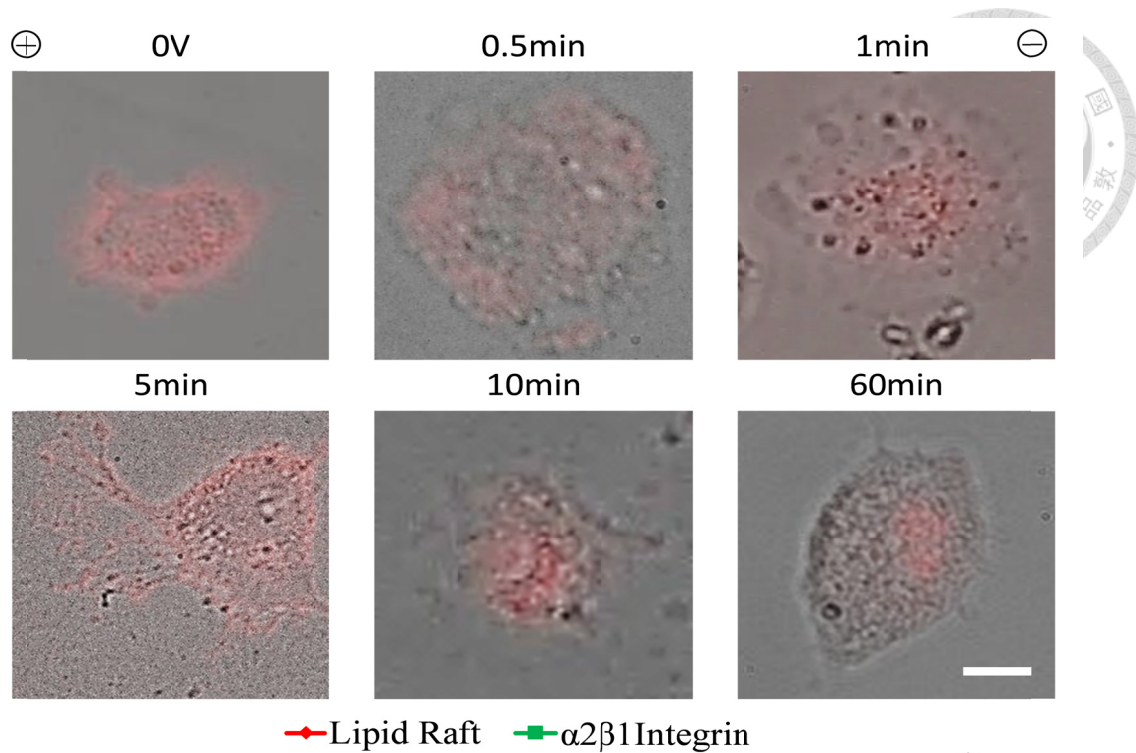


Figure 4. Lipid raft polarization

Lipid raft labeled with CTxB polarized gradually at cathodal side of fibroblasts and significantly till electric field stimulates fibroblasts for 60 minutes. (* $P < 0.05$ Groups vs. 0V, n = 12-33)

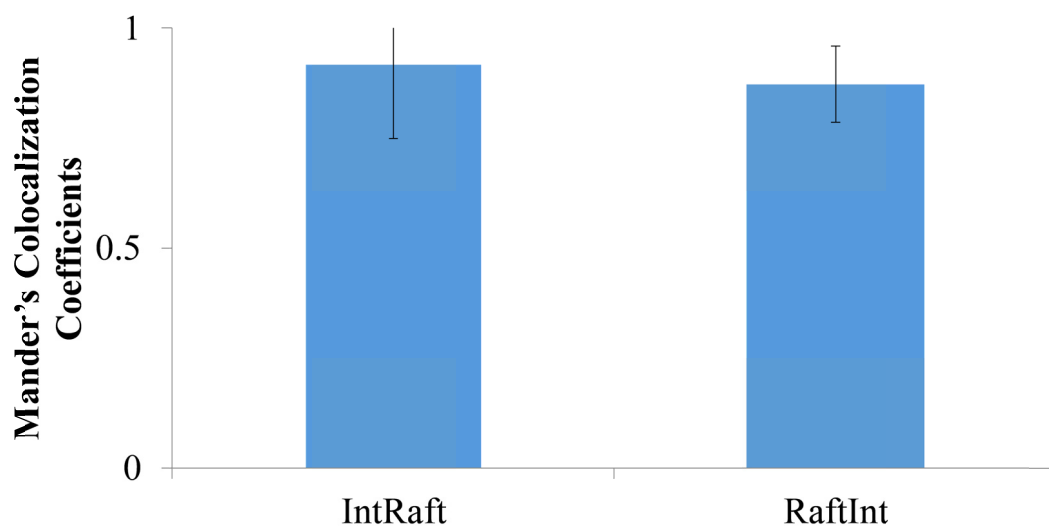
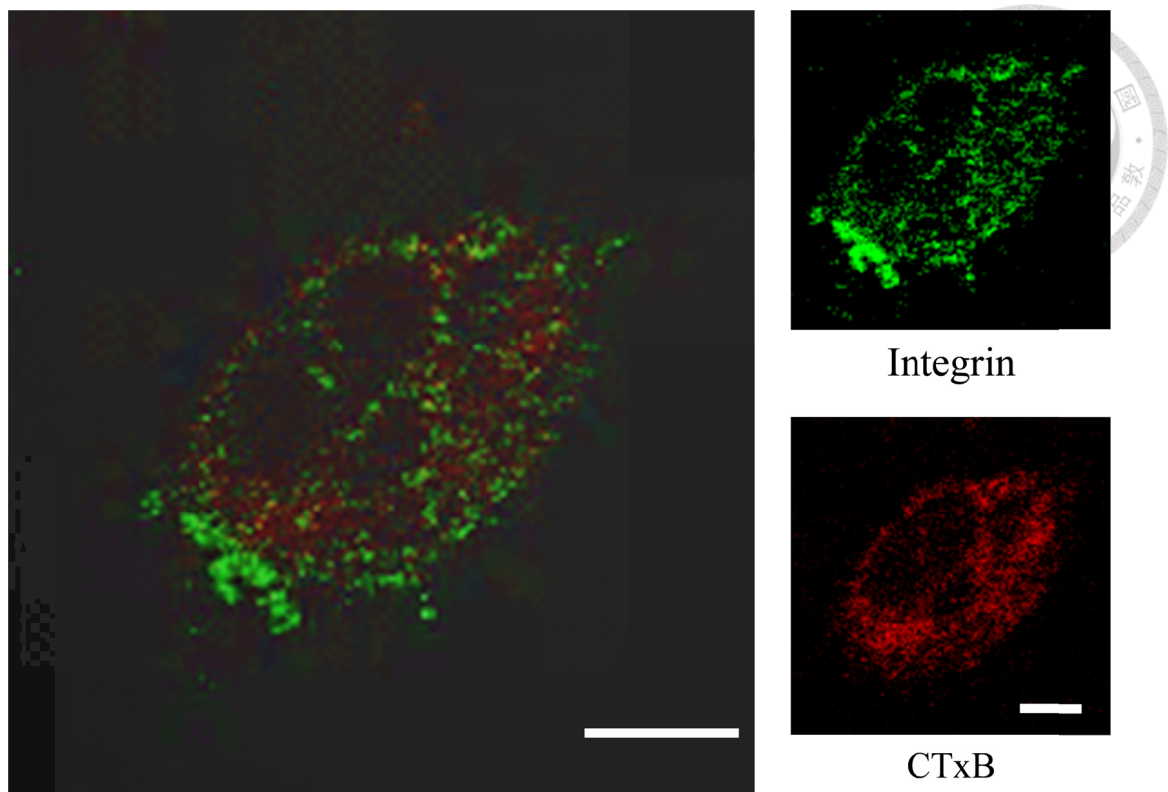


Figure 5. Coincide between lipid raft and $\alpha 2\beta 1$ integrin

IntRaft means $\alpha 2\beta 1$ integrin located on lipid raft, *vice versa*. Green signal representing $\alpha 2\beta 1$ integrin colocalize with red, lipid raft. According to Mander's colocalization coefficient, 92% $\alpha 2\beta 1$ integrin locate on lipid raft and 87% lipid raft locate on $\alpha 2\beta 1$ integrin.

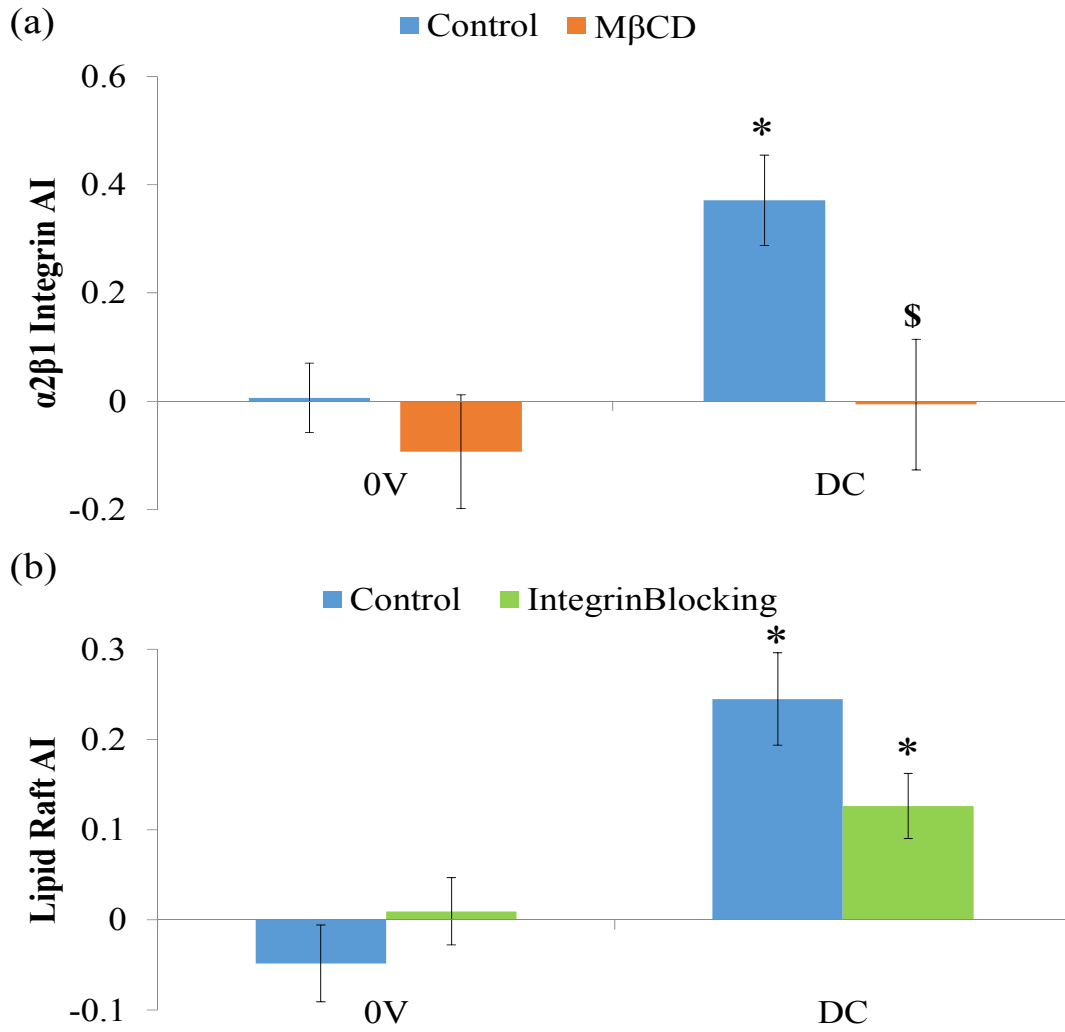


Figure 6. $\alpha 2\beta 1$ integrin riding lipid raft

(a) Electric field induces the AI increase of $\alpha 2\beta 1$ integrin and M β CD impair that. (b)

Anti- $\alpha 2\beta 1$ integrin antibody blocks the integrin function but does not affect the AI of

lipid raft. (* $P < 0.05$ DC vs. 0V, \$ $P < 0.05$ Groups vs. Control, $n = 21-50$)

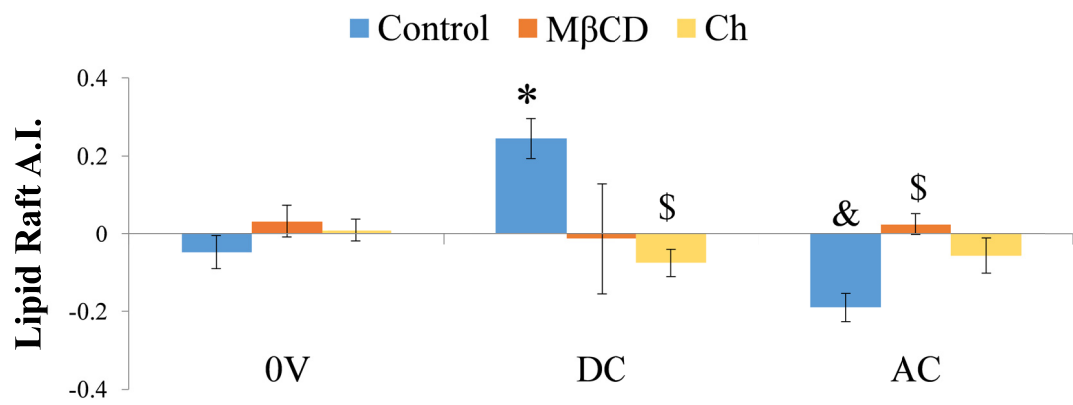
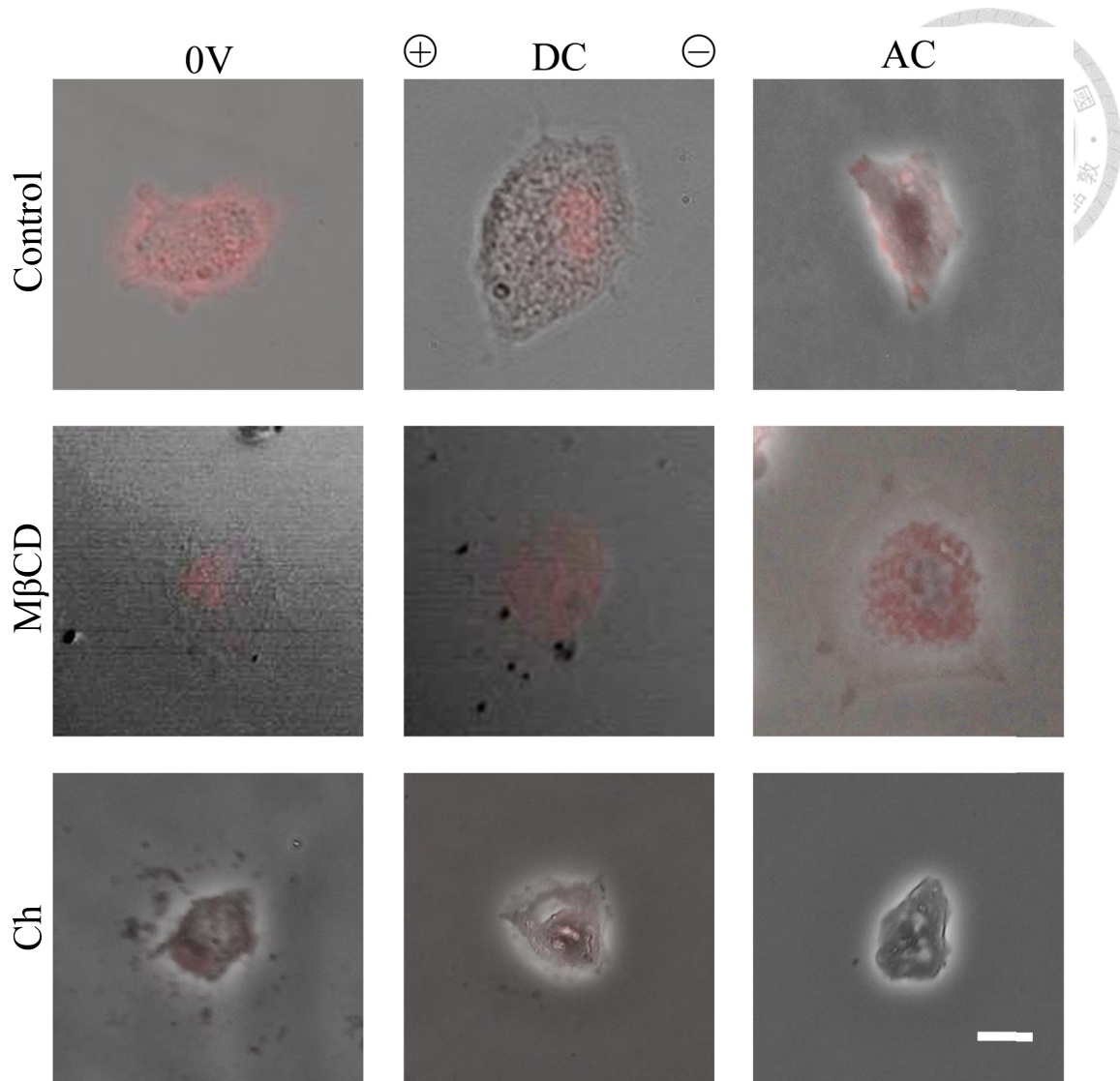
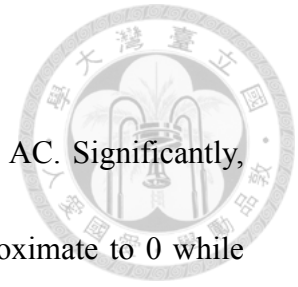


Figure 7. Lipid raft polarization disrupt by Ch and M β CD

The asymmetric distribution (AI) of lipid raft results from DC or AC. Significantly, the AI of DC drop while treated with Ch and the AI of AC approximate to 0 while treated with M β CD (* P < 0.05 Groups vs. 0V , \$ P < 0.05 Groups vs. Control , & P<0.05 Groups vs. DC, n = 17-118).



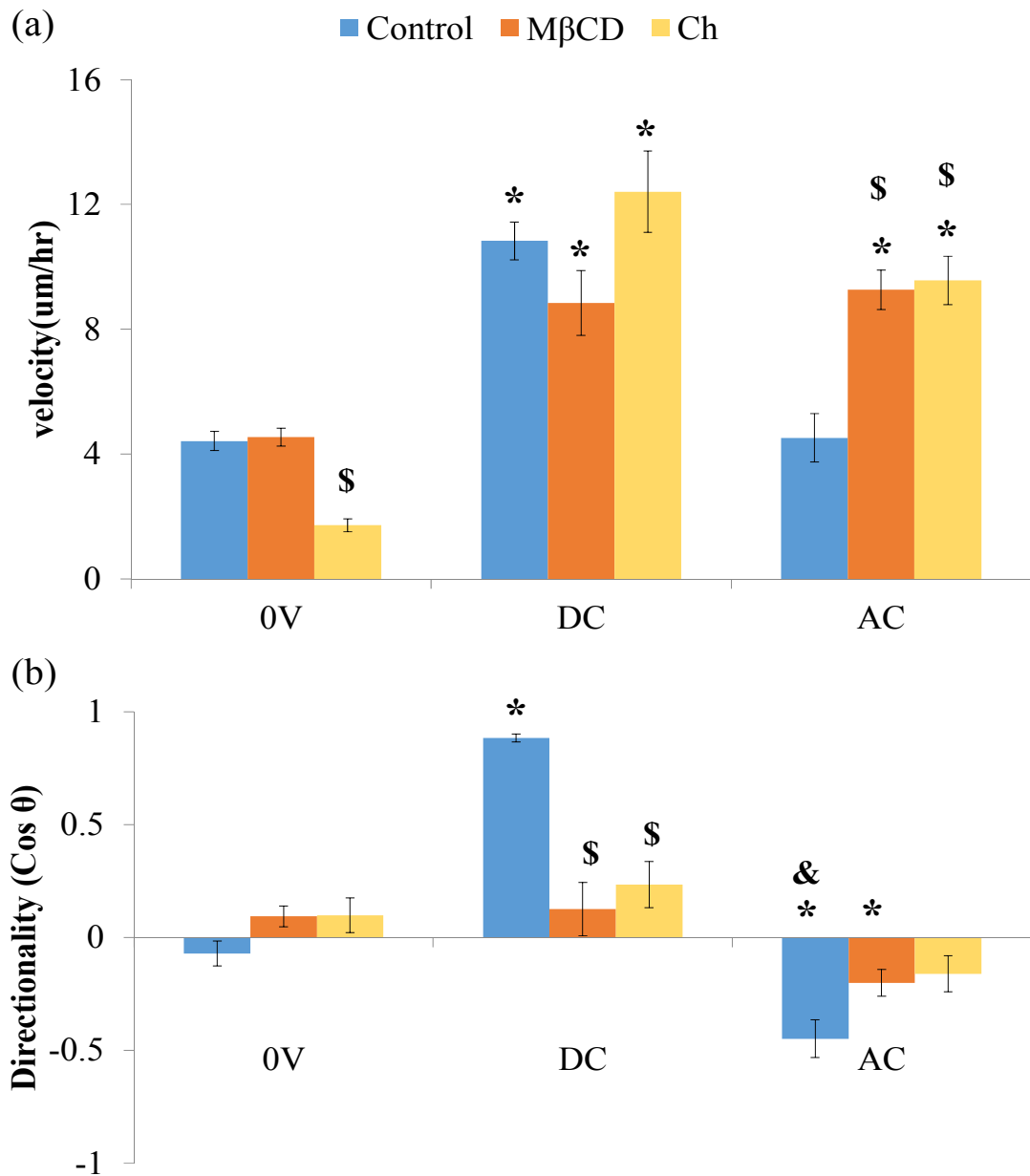
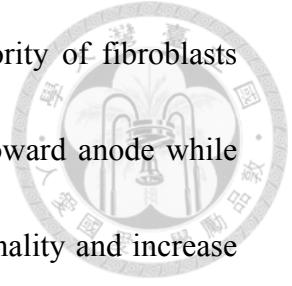


Figure 8. Ch and MβCD impair galvanotaxis

(a) DC EF stimulation enhances the fibroblasts' migration speed but AC shows not difference with 0V. No significant difference between control and the groups treated with MβCD or Ch when fibroblasts exposed on 6V/cm. However, MβCD or Ch improve the velocity simulated by AC. It seems that MβCD or Ch could enhance cell performance induced by AC. (b) The directionality simulated by DC is higher than 0V

and by AC is more negative than 0V. It represents that the majority of fibroblasts migrate toward cathode while DC electric field stimulation and toward anode while exposed on AC. The MβCD and Ch could reduce the DC directionality and increase the AC directionality. Therefore, pharmaceutical treatments inhibit directional migration induced by DC or AC. (* P < 0.05 Groups vs. 0V, \$ P < 0.05 Groups vs. Control, & P<0.05 Groups vs. DC, n = 42-171)



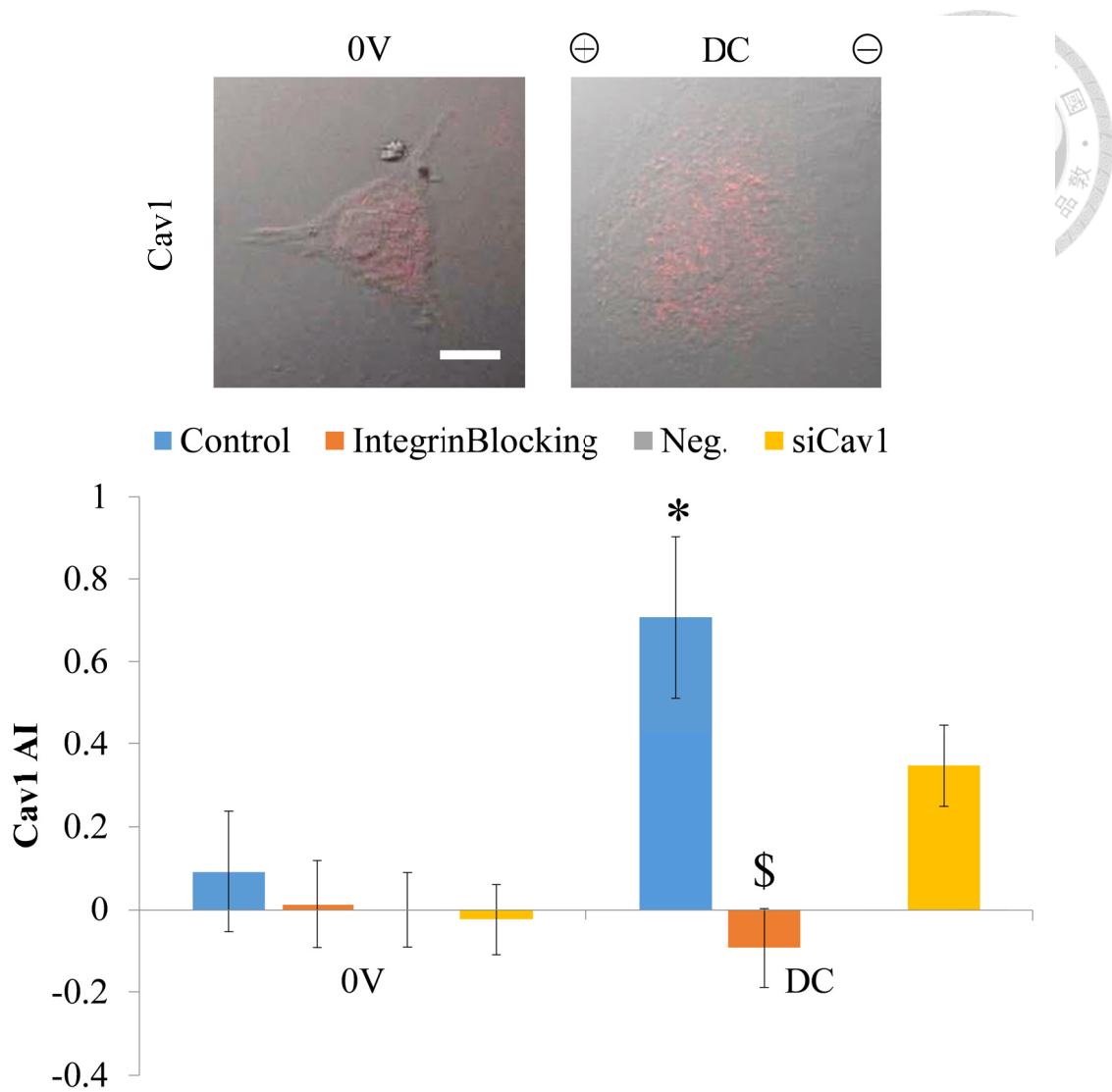


Figure 9. Cav1 polarize under electric field stimulation.

The IF images show the majority of red signal, caveolin-1, distribute at cathodal side.

The functional block on $\alpha2\beta1$ integrin decrease caveolin-1 AI but the knockdown on caveolin-1 show no affect. (* $P < 0.05$ Groups vs. 0V, \$ $P < 0.05$ Groups vs. Control,

n = 14-42)

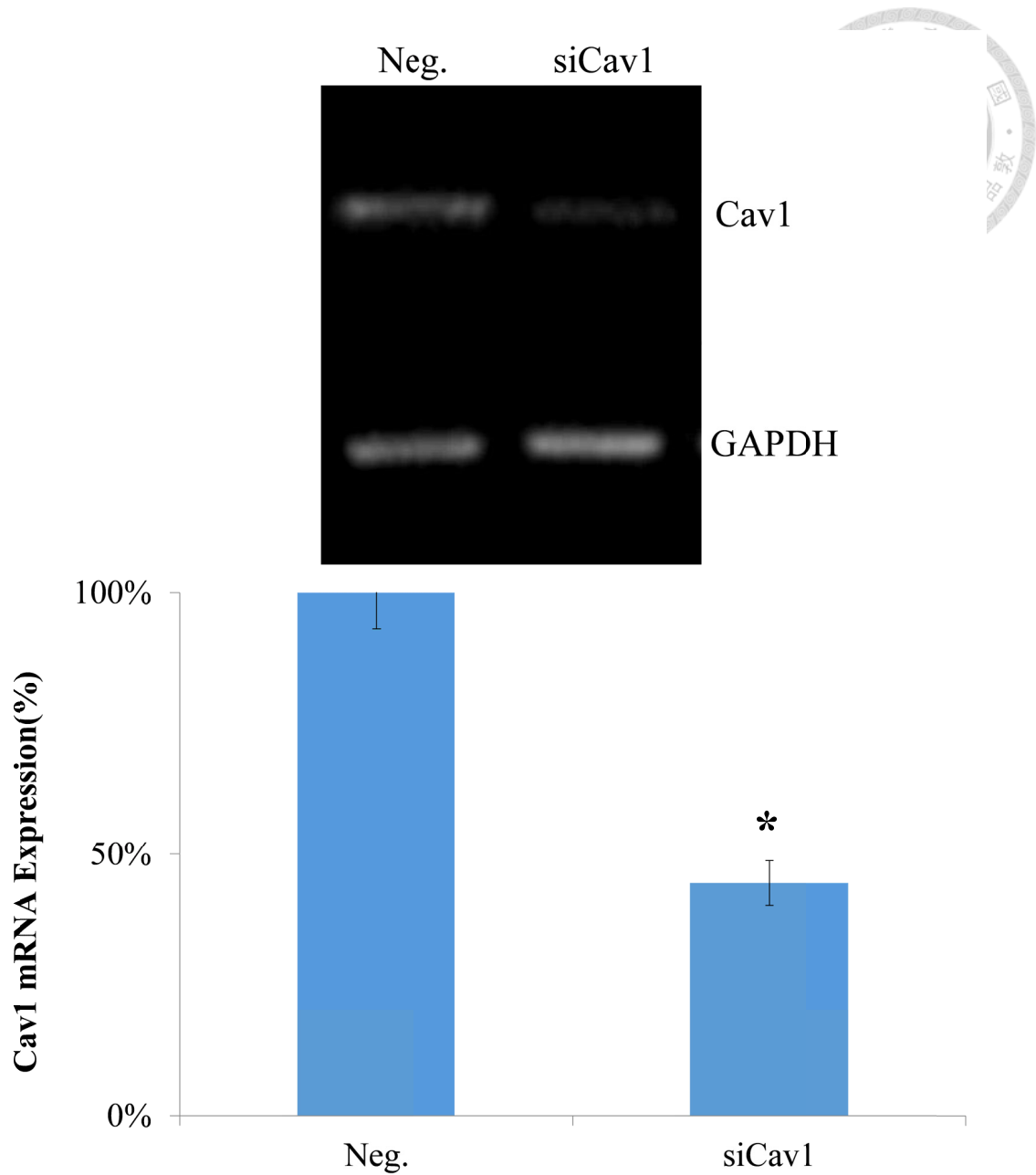


Figure 10. Cav1 knockdown by RNAi.

Gene expression level represents the light intensity of band using by PCR. The siRNA, targeting to caveolin-1, decrease a half expression level of caveolin-1 than control. (*

$P < 0.05$ Groups vs. Control)

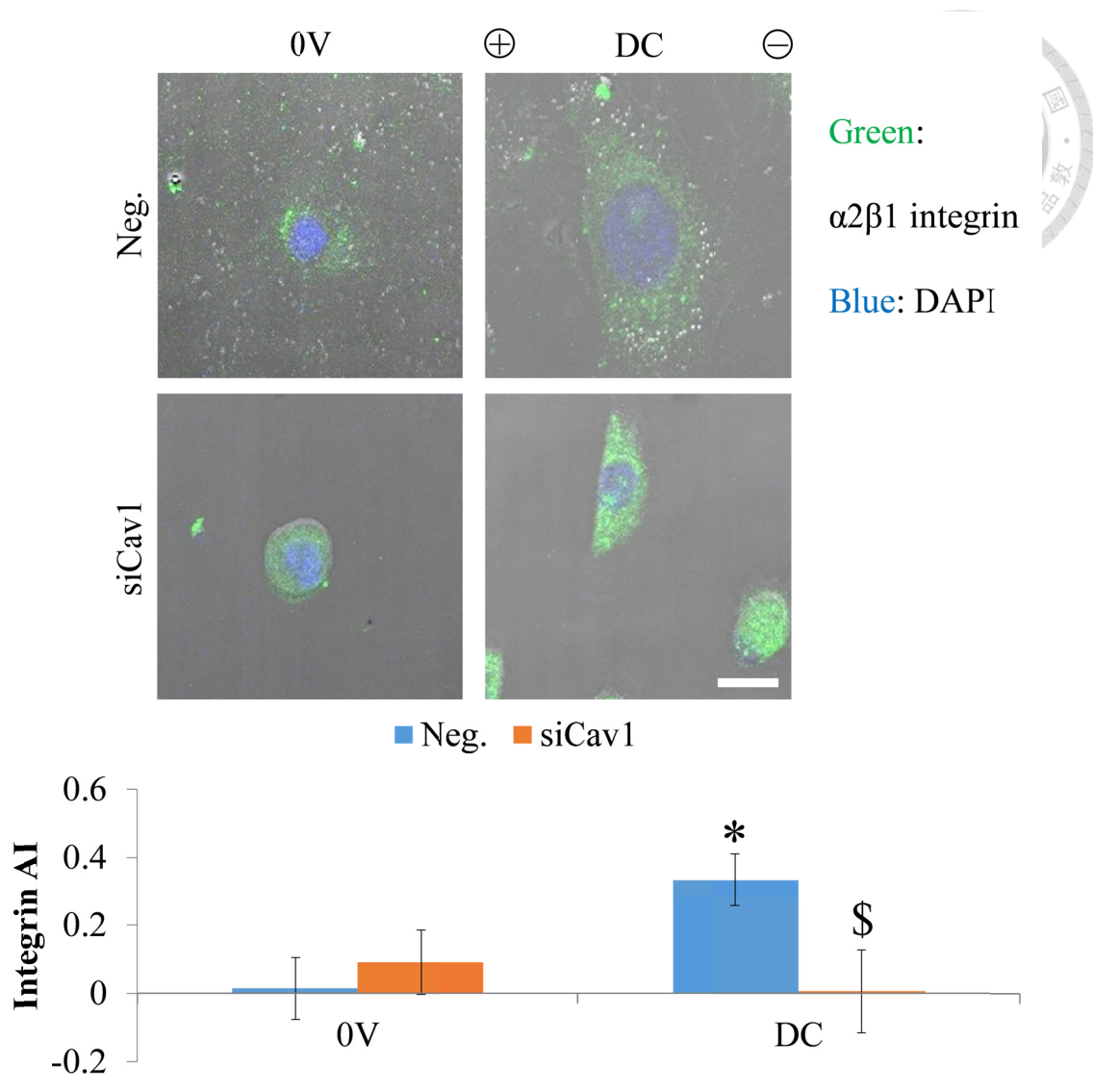


Figure 11 Caveolin-1 knockdown disrupt $\alpha 2\beta 1$ integrin distribution

Fibroblasts with caveolin-1 knockdown show lower integrin AI than negative control.

(* $P < 0.05$ Groups vs. 0V, \$ $P < 0.05$ Groups vs. Control, n = 20-26)

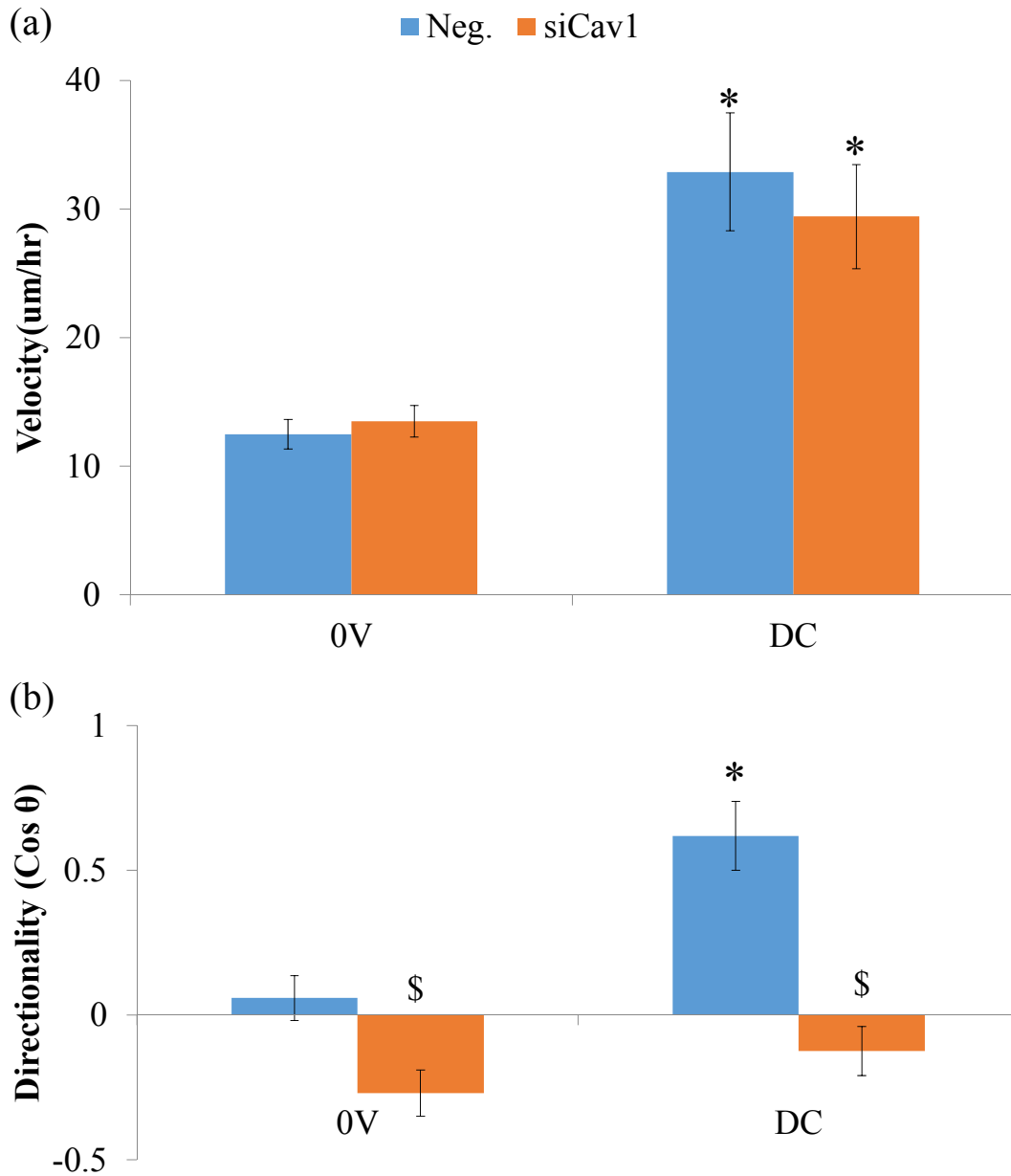


Figure 12. Cav1 knockdown reduce directionality.

(a) Fibroblasts increase their migration velocity whether or not the caveolin-1 knockdown. The expression level of caveolin-1 do not alters cell motility.

(b) Caveolin-1 knockdown inhibit the directionality. (* $P < 0.05$ Groups vs. 0V, \$ $P < 0.05$ Groups vs. Control, n = 40-95)

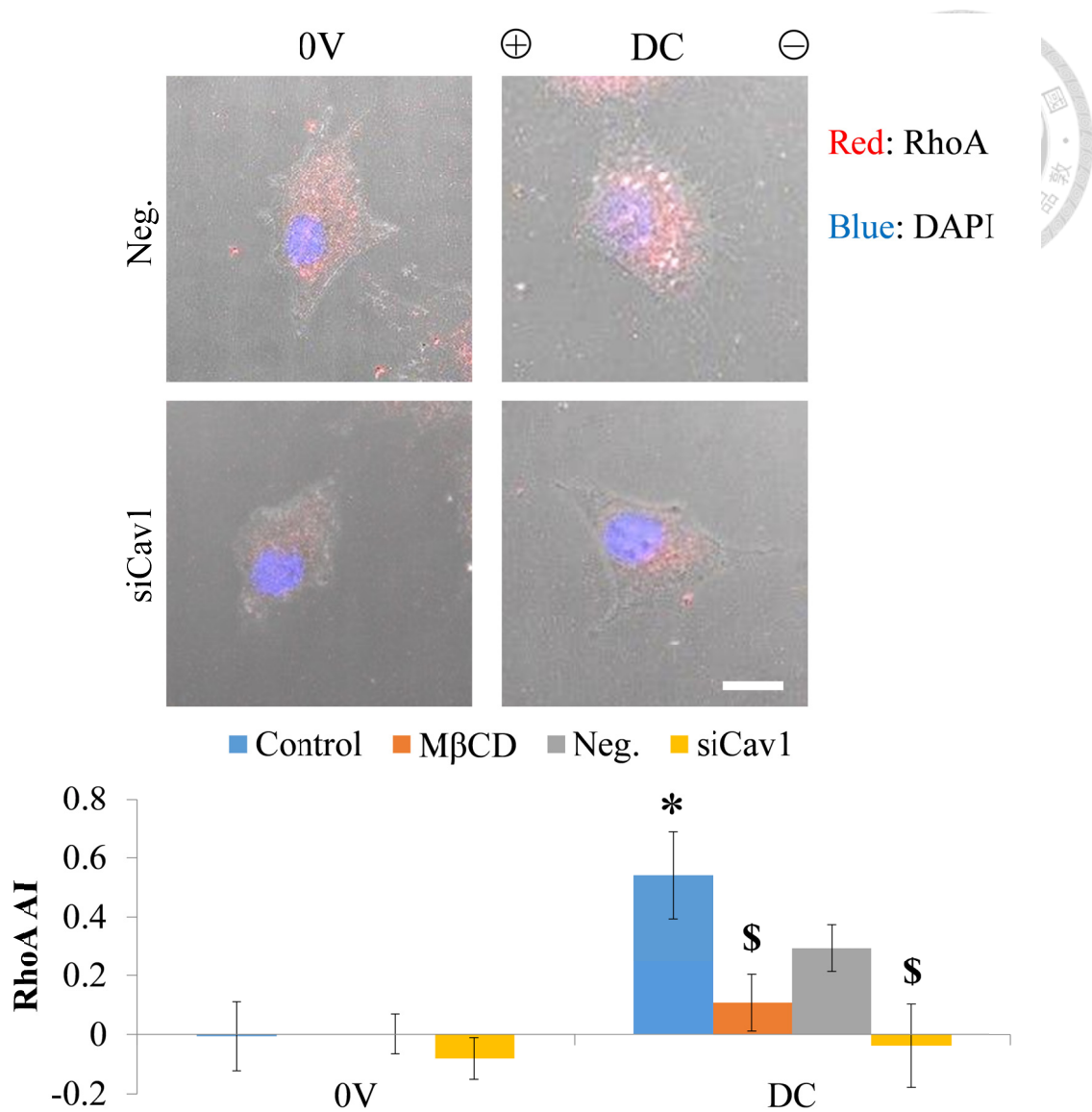
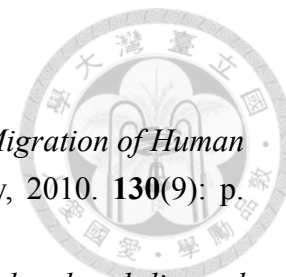


Figure 13. RhoA polarization induced by EF is impaired by RNAi.

RhoA polarize at cathode and AI of RhoA increase while cell exposed to electric field compared to the negative control. The MβCD and siRNA for caveolin-1 reduce the AI of RhoA. (\$ P < 0.05 Groups vs. Control, n = 4-30)

Reference



1. Guo, A., et al., *Effects of Physiological Electric Fields on Migration of Human Dermal Fibroblasts*. Journal of Investigative Dermatology, 2010. **130**(9): p. 2320-2327.
2. Song, B., *Nerve regeneration and wound healing are stimulated and directed by an endogenous electrical field in vivo*. Journal of Cell Science, 2004. **117**(20): p. 4681-4690.
3. Sun, Y.-S., S.-W. Peng, and J.-Y. Cheng, *In vitro electrical-stimulated wound-healing chip for studying electric field-assisted wound-healing process*. Biomicrofluidics, 2012. **6**(3): p. 034117-12.
4. Zhao, M., *Electrical fields in wound healing-An overriding signal that directs cell migration*. Semin Cell Dev Biol, 2009. **20**(6): p. 674-82.
5. Zhao, M., et al., *Electrical signals control wound healing through phosphatidylinositol-3-OH kinase-[gamma] and PTEN*. Nature, 2006. **442**(7101): p. 457-460.
6. Chao, P.-h.G., et al., *Effects of Applied DC Electric Field on Ligament Fibroblast Migration and Wound Healing*. Connective Tissue Research, 2007. **48**(4): p. 188-197.
7. Allen, Greg M., A. Mogilner, and Julie A. Theriot, *Electrophoresis of Cellular Membrane Components Creates the Directional Cue Guiding Keratocyte Galvanotaxis*. Current Biology, 2013(0).
8. Cho, M.R., et al., *Induced redistribution of cell surface receptors by alternating current electric fields*. The FASEB Journal, 1994. **8**(10): p. 771-6.
9. Tsai, C.-H., B.-J. Lin, and P.-H.G. Chao, *$\alpha 2\beta 1$ integrin and RhoA mediates electric field-induced ligament fibroblast migration directionality*. Journal of Orthopaedic Research, 2012.
10. Zhao, M., et al., *Membrane lipids, EGF receptors, and intracellular signals colocalize and are polarized in epithelial cells moving directionally in a physiological electric field*. The FASEB Journal, 2002.
11. Han, J., et al., *Integrin beta1 subunit signaling is involved in the directed migration of human retinal pigment epithelial cells following electric field stimulation*. Ophthalmic Res, 2011. **45**(1): p. 15-22.
12. Jonathan D. Humphries, A.B., Martin J. Humphries, *Integrin ligands at a glance*. Journal of Cell Science, 2006. **119**: p. 3901-3903.
13. Palazzo, A.F., et al., *Localized Stabilization of Microtubules by Integrin- and FAK-Facilitated Rho Signaling*. Science, 2004. **303**(5659): p. 836-839.
14. Ann M. Rajnicek, L.E.F., Colin D. McCaig, *Temporally and spatially*

- coordinated roles for Rho, Rac, Cdc42 and their effectors in growth cone guidance by a physiological electric field.* Journal of Cell Science, 2006. **119**: p. 1723-1735.
15. Burdisso, J.E., Á. González, and C.O. Arregui, *PTP1B promotes focal complex maturation, lamellar persistence and directional migration.* Journal of Cell Science, 2013. **126**(8): p. 1820-1831.
16. Guilluy, C., R. Garcia-Mata, and K. Burridge, *Rho protein crosstalk: another social network?* Trends in Cell Biology, 2011. **21**(12): p. 718-726.
17. Pike, L.J., *Rafts defined: a report on the Keystone symposium on lipid rafts and cell function.* The Journal of Lipid Research, 2006. **47**(7): p. 1597-1598.
18. Hernandez-Deviez, D.J., et al., *Caveolin regulates endocytosis of the muscle repair protein, dysferlin.* Journal of Biological Chemistry, 2008. **283**(10): p. 6476-6488.
19. Wickström, S.A. and R. Fässler, *Regulation of membrane traffic by integrin signaling.* Trends in Cell Biology, 2011. **21**(5): p. 266-273.
20. Sotobori, T., et al., *Bone morphogenetic protein-2 promotes the haptotactic migration of murine osteoblastic and osteosarcoma cells by enhancing incorporation of integrin beta1 into lipid rafts.* Exp Cell Res, 2006. **312**(19): p. 3927-38.
21. Kusumi, A. and K. Suzuki, *Toward understanding the dynamics of membrane-raft-based molecular interactions.* Biochimica et Biophysica Acta (BBA) - Molecular Cell Research, 2005. **1746**(3): p. 234-251.
22. Leitinger, B. and N. Hogg, *The involvement of lipid rafts in the regulation of integrin function.* Journal of Cell Science, 2002. **115**(5): p. 963-972.
23. Cécile Boscher, I.R.N., *Caveolins and Caveolae: Roles in Signaling and Disease Mechanisms*, in *CAVEOLIN-1: Role in Cell Signaling*, Jean-François Jasmin, Philippe G. Frank, and Michael P. Lisanti, Editors. 2012.
24. Yang, B., et al., *p190 RhoGTPase-Activating Protein Links the β 1 Integrin/Caveolin-1 Mechanosignaling Complex to RhoA and Actin Remodeling.* Arteriosclerosis, Thrombosis, and Vascular Biology, 2010. **31**(2): p. 376-383.
25. Rey-Barroso, J., et al., *The dioxin receptor controls β 1 integrin activation in fibroblasts through a Cbp-Csk-Src pathway.* Cellular Signalling, 2013. **25**(4): p. 848-859.
26. Beardsley, A., et al., *Loss of caveolin-1 polarity impedes endothelial cell polarization and directional movement.* Journal of Biological Chemistry, 2005. **280**(5): p. 3541-3547.
27. Arpaia, E., et al., *The interaction between caveolin-1 and Rho-GTPases*

- promotes metastasis by controlling the expression of alpha5-integrin and the activation of Src, Ras and Erk.* Oncogene, 2012. **31**(7): p. 884-896.
28. Feng, C.-h., Y.-c. Cheng, and P.-h.G. Chao, *The influence and interactions of substrate thickness, organization and dimensionality on cell morphology and migration.* Acta Biomaterialia, 2013. **9**(3): p. 5502-5510.
29. Danthi, P. and M. Chow, *Cholesterol Removal by Methyl-β-Cyclodextrin Inhibits Poliovirus Entry.* Journal of Virology, 2003. **78**(1): p. 33-41.
30. Carmena, M.J., et al., *Cholesterol modulation of membrane fluidity and VIP receptor/effector system in rat prostatic epithelial cells.* Regul Pept, 1991. **33**(3): p. 287-97.
31. Hart, F.X., et al., *Keratinocyte galvanotaxis in combined DC and AC electric fields supports an electromechanical transduction sensing mechanism.* Bioelectromagnetics, 2013. **34**(2): p. 85-94.
32. Berdeaux, R.L., et al., *Active Rho is localized to podosomes induced by oncogenic Src and is required for their assembly and function.* J Cell Biol, 2004. **166**(3): p. 317-23.
33. Tandon, N., et al., *Electrical stimulation systems for cardiac tissue engineering.* Nat. Protocols, 2009. **4**(2): p. 155-173.